Journal of Molecular Structure 1087 (2015) 51–59

Contents lists available at ScienceDirect

Journal of Molecular Structure

journal homepage: www.elsevier.com/locate/molstruc

Vibrational spectroscopic studies of N1-ethyl-5′-bromo-7-azaindirubin-3′-oxime and N1-ethyl-indirubin-3′-monooxime

Ying-Sing Li [a,*], Qi-Zheng Yao [b], Zhao-Hui Wang [b], Jingcai Cheng [c], Tuyen Thi T. Truong [a]

[a] Department of Chemistry, University of Memphis, Memphis, TN 38152, USA
[b] School of Pharmacy, China Pharmaceutical University, Nanjing 210009, China
[c] JC (Wuxi) COMPANY, Inc., Wuxi, JS 214036, China

HIGHLIGHTS

- The title compounds were synthesized and identified.
- These compounds were studied by vibrational spectroscopy.
- Vibrational assignments were suggested based on the previous work and the group characteristic frequencies.
- Thermal analyses were conducted by DSC and temperature variation of IR spectra.

ARTICLE INFO

Article history:
Received 12 November 2014
Received in revised form 15 January 2015
Accepted 20 January 2015
Available online 29 January 2015

Keywords:
N1-ethyl-5′-bromo-7-azaindirubin-3′-oxime
N1-ethyl-indirubin-3′-monooxime
Indirubin
Raman spectra
IR spectra
Thermal stability

ABSTRACT

We have prepared N1-ethyl-5′-bromo-7-azaindirubin-3′-oxime due to its potential for being a pharmaceutical. Infrared and Raman spectra have been recorded and vibrational assignments have been suggested based mainly on our previous vibrational investigation of N1-isopropyl-5′-chloro-7-azaindirubin-3′-oxime and on group characteristic frequencies. Temperature variation study has revealed the presence of conformers due to the internal rotation of ethyl group. IR spectra collected for N1-ethyl-7-azaindirubin-3′-oxime have shown rather similar spectral features with that of N1-ethyl-5′-bromo-7-azaindirubin-3′-oxime. IR spectra of these compounds have revealed the association through hydrogen bonding in the solid state. IR spectra recorded for these samples after annealing at high temperatures indicated the thermal conversion temperature to be lowered than 270 °C. Results from thermal analyses have determined the beginning decomposition temperatures to be 250 °C and the decomposition enthalpies to be 94 kJ/mol for both N1-ethyl-5′-bromo-7-azaindirubin-3′-oxime and N1-ethyl-7-azaindirubin-3′-oxime.

Introduction

Indirubin is an active ingredient in a traditional Chinese herbal medicine, used in the treatment of chronic myelogenous leukemia. It was reported that the compound could be helpful for treating glioblastoma – a deadly brain tumors [1]. It has also been found to exhibit antileukemic effectiveness in chronic myelocytic leukemia [2]. The crystal structure of cyclin-dependent kinases-2 (CDK-2) in complex with indirubin derivatives shows that indirubin interacts with the kinase's ATP-binding site through van der Waals interactions and three hydrogen bonds [3]. Due to the high affinity with the enzymes ATP binding site, indirubin and some of its derivatives have potent inhibitory potential toward CDKs [4–6]. Histological and transmission electron microscopic (TEM) investigations indicate that indirubin-3-monoxime has antitumor effect [7].

Perpete et al. have evaluated the UV/Vis spectra of a series of indirubin, isoindigo and other indigo/thio related dyes by using time-dependent Density Function Theory (DFT) in conjunction with the polarizable continuum model [8]. Results from the electrochemical and IR spectroscopic studies on the interaction of indirubin with DNA show that indirubin interacts with phosphate group of DNA by hydrogen bond or electrostatic interaction [9]. Karapanayiotis et al. have considered the influence of various halogen on the Raman spectrum in their Raman spectroscopic studies of indigo and its four 6,6′-halogeno analogues [10].

The purpose of the present work is to study the vibrational spectra of indirubin derivatives and their thermal stabilities. It is

* Corresponding author. Tel.: +1 901 678 2621; fax: +1 901 678 3447.
E-mail address: yingli@memphis.edu (Y.-S. Li).

http://dx.doi.org/10.1016/j.molstruc.2015.01.036
0022-2860/

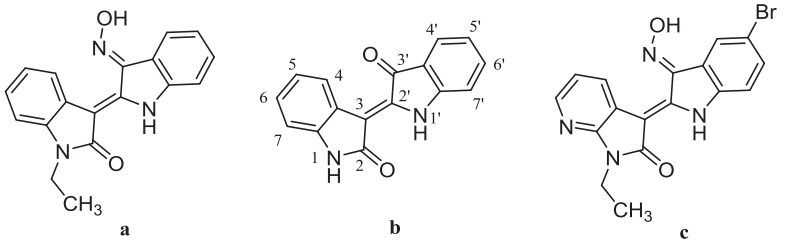

Scheme 1. Structural formulas of (a) EIM, (b) indirubin and (c) EBAIO.

expected that the vibrational spectroscopy can provide useful information about the characteristics and stabilities of the active component or its derivatives of a drug. It has recently been reviewed that Raman scattering is a useful spectroscopic method in the study of pharmaceuticals [11]. Due to the potential in pharmaceutical applications, we had recorded the surface enhanced Raman scattering (SERS) of N1-ethyl indirubin-3′-monooxime (EIM) by using a silver coated microscopic slide pre-treated with indium tin oxide nanopowder [12]. The use of the oxide nanopower for the pretreatment was to improve the surface morphology of the product substrate for better Raman signal enhancement. From the observed SERS bands and their vibrational assignments, it is unlikely that the molecules absorbed horizontally on silver surface through aromatic π-electrons. Result from this study suggested that EIM interacted with the substrate through the lone pair electrons of the oxime functional group. Our recent vibrational spectroscopic investigation of N1-isopropyl-5′-chloro-7-azaindirubin-3′-oxime (ICAIO) revealed that the molecule has a planar ring structure with a bisecting isopropyl functional group that includes an eclipsed secondary C—H (Cl_2—Cl_2H) bond with the N1—C bond. Vibrational assignments were suggested based essentially on the results from DFT calculations [13]. As a continuation of our investigation of indirubin derivations, we have carried out the vibrational spectroscopic study on N1-ethyl-5′-bromo-7-azaindirubin-3′-oxime (EBAIO). As there is a close similarity of molecular structure between ICAIO and EBAIO, it would be reasonable to suggest the vibrational assignments, based essentially on the vibrational characteristics of ICAIO. Additionally, we have recorded infrared (IR) spectra of EIM and carried out thermal analyses for ICAIO, EBAIO and EIM. Scheme 1 shows the molecular structural formulas of EBAIO, EIM and indirubin. The analogue of molecular structure between EBAIO and EIM might suggest some similarities in their vibration spectral features.

Experimental

Unless noted, all solvents and reagents were freshly distilled or purified according to standard procedures. Indirubin was purchased from Nanjing Zelang Pharmaceutical Technology Co. Ltd.; it was purified by crystallization in acetone.

Melting points were taken on XT-4 micro melting point apparatus and are uncorrected. Analytical TLC was carried out with plates pre-coated with silica gel 60 F254 (0.25 mm thick) and visualized under UV lamp (254 nM). Flash column chromatography was carried out on silica-gel 200–300 mesh.

Preparation of EBAIO(c)

There are two major steps in the preparation of EBAIO. The first step is involved with the synthesis of N1-ethyl-5′-bromo-7-azaindirubin (EBAI) from the reaction between N1-ethyl-7-azaindole-2,3-dione and 1-acetyl-3-hydroxy-5-bromoindole.The second step is the oximation of EBAI. The experimental detail for the sample preparation is given in the following:

Step 1: Synthesis of EBAI

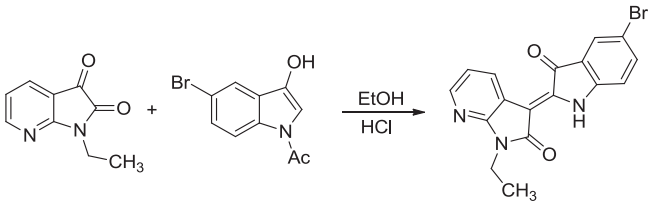

To a solution of N1-ethyl-7-azaindole-2,3-dione (0.22 g, 1.23 mmol) and 1-acetyl-3-hydroxy-5-bromoindole (0.31 g, 1.23 mmol) in ethanol (20 mL), several drops of concentrated hydrochloric acid were added until pH = 1–2 [14]. The mixture was stirred at 60–65 °C for 1 h [15]. The reaction mixture was cooled down and filtered, and the filtrate was distilled to remove the ethanol. The obtained residue was dissolved with chloroform and the solution was washed with water for several times, and concentrated to afford EBAI. The crude product was then purified by column chromatography (200–300 mesh silica gel; chloroform/ligroin, 3:1, v/v) followed by recrystallization in acetone to get 0.24 g red needle-like crystal powder (yield: 52%); mp: 249–251 °C(des.).

IR (KBr, í, cm^{-1}): 3432, 3319, 3139, 1654, 1594, 1456, 1400, 1384, 1205, 1101, 970; ^{1}H nuclear magnetic resonance (NMR) (300 MHz, $CDCl_3$, ppm) δ: 1.37 (t, 3H, *J* = 7.14 Hz, CH_3), 4.03 (q, 2H, *J* = 7.14 Hz, N—CH_2), 6.93 (d, 1H, *J* = 8.46 Hz, 7′-H), 7.05 (dd, 1H, *J* = 5.21, 7.68 Hz, 5-H), 7.63 (dd, 1H, *J* = 2.03, 8.46 Hz, 6′-H), 7.85 (d, 1H, *J* = 2.03 Hz, 4′-H), 8.21 (dd, 1H, *J* = 1.57, 5.21 Hz, 6-H), 8.97 (dd, 1H, *J* = 1.57, 7.68 Hz, 4-H), 10.43 (s, 1H, N′—H); ESI-MS (*m*/*z*) $[M+H]^+$: 370.0 (Br = 79), 372.0 (Br = 81). Anal. Calcd. (%) for $C_{17}H_{12}BrN_3O_2$ (369.2): C, 55.16; H, 3.27; N, 11.35; Found (%): C, 55.24; H, 3.33; N, 11.27.

Step 2: Synthesis of EBAIO

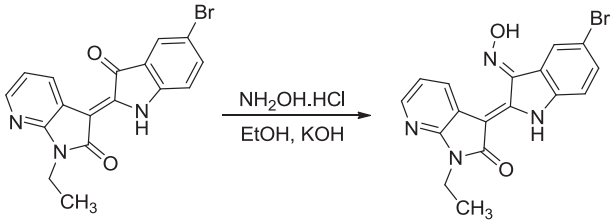

0.3 g of hydroxylamine hydrochloride and 0.6 g KOH were added to a solution of 0.24 g EBAI (0.64 mmol) in ethanol (10 mL). The reaction mixture was stirred at room temperature for 0.5 h, and then poured into water. The mixture was neutralized with glacial acetic acid and the formed precipitate was filtrated and washed with water to provide 0.24 g EBAIO (yield: 98%), an orange crystal powder; mp: 288–289 °C(des.). 1H NMR (300 MHz, CDC_{l3}, ppm) δ:1.25 (t, 3H, *J* = 6.87 Hz, CH_3), 3.93 (q, 2H, *J* = 6.87 Hz, N—CH_2), 7.03 (dd, 1H, *J* = 5.26, 7.59 Hz, 5-H), 7.44 (d, 1H, *J* = 8.39 Hz, 7′-H), 7.62 (d, 1H, *J* = 8.39 Hz, 6′-H), 8.10 (d, 1H, *J* = 5.26 Hz, 6-H), 8.31 (s, 1H, 4′-H), 8.79 (d, 1H, *J* = 7.59 Hz,

4-H), 11.74 (s, 1H, N′-H), 13.94 (s, 1H, NOH); ESI-MS *m/z* [M−H]-: 383.1 (Br = 79), 385.1 (Br = 81). Anal. Calcd. (%) for $C_{17}H_{13}BrN_4O_2$. ¼ H_2O (389.72): C, 52.39; H, 3.49; N, 14.39. Found (%): C, 51.89; H, 3.73; N, 13.86.

Preparation of EIM(a)

There are two major steps in the preparation of EIM. The first step is involved with the synthesis of N1-ethylindirubin (EI) from the reaction between indirubin and ethyl iodide. The second step is the preparation of EIM *via* the oximation of EI.

Step 1: Synthesis of EI

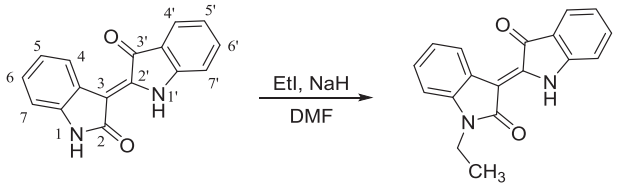

2.62 g (10 mmol) of indirubin were treated with 0.6 g (15 mmol) of NaH at 0 °C in 40 mL of anhydrous *N,N*-dimethylformamide (DMF), and subsequently 1.15 mL(15 mmol) of ethyliodide (EtI) in 5 mL anhydrous DMF were slowly added drop wise. The resulting solution was stirred at room temperature. After the reaction was completed (TLC checking petroleum ether/ethyl acetate = 3/1), the reaction mixture was poured into water (~300 mL). The product was extracted with dichloromethane three times (150 mL × 3) and the combined organic layers were dried over Na_2SO_4. The concentrated crude product was purified by silica-gel column chromatography with petroleum ether/ethylacetate (4/1) as eluent to afford 1.5 g of EI (yield: 52%), an purple crystal powder; mp: >200 °C(des.); ^{1}H NMR(300 MHz, $CDCl_3$, ppm) δ: 1.33(t, *J* = 7.25 Hz, 3H, CH_3), 3.89(q, *J* = 7.24 Hz, 2 H, CH_2), 6.87–6.90 (m, 1H, H-Ph), 6.94–6.98 (m, 1H, H-Ph), 7.00–7.02 (m, 1H, H-Ph), 7.11–7.13 (m, 1H, H-Ph), 7.27–7.29 (m, 1H, H-Ph), 7.52 (d, *J* = 7.60 Hz, 1H, H-Ph), 7.74(d, *J* = 7.60 Hz, 1H, H-Ph), 8.90(d, *J* = 7.60 Hz, 1H, H-Ph), 10.56(bs, 1H, NH-1); ESI-MS (*m/z*):291.2 $[M+H]^+$; Anal. Calcd (%) for $C_{18}H_{14}N_2O_2$(290.32): C 74.47, H 4.86, N 9.65; Found (%): C 74.33, H 4.85, N 9.41.

Step 2: Synthesis of EIM

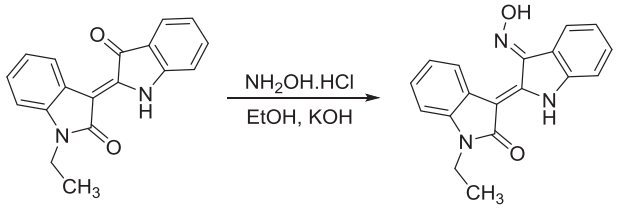

The preparation process of EIM is similar to that of BEAIO. Using 1.2 g of EI (2.9 mmol) as starting material, 0.65 g EIM were obtained (yield 75%) as an orange crystal powder; mp: >200 °C(des.); 1H NMR(300 MHz, CD_3COCD_3, ppm) δ: 1.28 (t, *J* = 7.25 Hz, 3H, CH_3), 3.94 (q, *J* = 7.25 Hz, 2 H, CH_2), 6.96–6.99 (m, 1H, H-Ph), 7.05–7.08 (m, 2H, H-Ph), 7.08–7.11 (m, 1H, H-Ph), 7.19–7.22 (m, 1H, H-Ph), 7.33–7.36 (m, 1H, H-Ph), 7.43–7.46(m, 1H, H-Ph), 8.38 (d, *J* = 7.82 Hz, 1H, H-Ph), 8.71 (d, *J* = 7.82 Hz, 1H, H-Ph), 10.56 (bs, 1H, NH-1); ESI-MS (*m/z*): 304.1 $[M-H]^-$; Anal. Calcd (%) for $C_{18}H_{15}N_3O_2$ (305.34): C, 70.81; H, 4.95; N, 13.76. Found (%): C, 70.56; H, 4.89; N, 13.87.

In the above sample preparations, instrumental methods for the identification of reaction intermediates and products were applied. Infrared (IR) spectra were performed on a Nicolet Avitar 370 DTGS infrared spectrophotometer; NMR spectra were recorded on Bruke AV-300 (300 MHz) NMR spectrometer using trimethylsilane (TMS) as an internal reference. The chemical shifts were reported in ppm (δ), and the coupling constants (*J*) were given in Hertz (Hz). Mass spectra (MS) were collected on Agilent 1100 LC/MS ESI (70–100 eV) mass spectrometer. Elemental analyses were carried out on an Elementar Vario EL instrument (Heraeus GmbH, Hanau, Germany).

For spectroscopic investigation, IR spectra were recorded in either adsorption or transmission mode by using a Matson Polaris FTIR spectrophotometer equipped with room temperature DTGS detector and WinFirst spectroscopy software. The IR sample was prepared by pressing each sample with KBr powder (IR grade, Sigma–Aldrich, St. Louis, MO, USA) to form pellets. The relative amount of sample was 3% by weight. For the low temperature investigation, a liquid nitrogen IR cell described in the previous study was applied [13]. A resolution of 2 cm^{-1} and a total of 96 scans were collected for each IR spectrum. Raman spectra were collected with a spectrophotometric system that consisted of a Spex Model 1403 double monochromator, a Melles Griot Omnischrome 43 argon ion laser, and a Hamamatsu Model R-928 photomultiplier tube. The 488 nm laser line was used as the excitation light source and the solid sample was filled in a capillary tube for Raman scattering measurements. In the Raman data collection, the resolution was set at 4 cm^{-1} and the laser power at the sample was 5–10 mW.

DSC plots were collected with a TA Q20 Differential Scanning Calorimeter (DSC). The system was purged with pure nitrogen at 50 mL/min and the heating rate was normally set at 5 °C/min.

Results and discussion

IR and Raman spectra of EBAIO

Our previous theoretical calculation has revealed that the most stable stereo isomer of ICAIO is in ZE form [13], in which the ring system linkage and the 3′-oxime functional group have cis (Z) and trans (E) forms, respectively. As EBAIO and ICAIO have identical ring system with different halogen substitutions at C5′ and different alkyl groups at N1, it is likely that the most stable stereoisomer of EBAIO is in ZE form. Similar to ICAIO, EBAIO is expected to have a highly conjugate ring system with all the heavy atoms in the rings and in the oxime and carbonyl groups sharing the same plane. This could be consistent with the potential function governing the twisted motion of the indoline and the pyrolidinone ring with respect to the C3=C2′. In case that the potential function is double minima, the ground vibrational state must have energy level higher than the barrier to the twist. Depending on the internal rotation of the ethyl group, EBAIO is expected to have either C_s or C_1 point group. In either case, all vibrational modes are both IR and Raman active.

Fig. 1 shows the FTIR and Raman spectra of EBAIO. In Fig. 1-B, a distinct Raman band at 1571 cm^{-1} has a much higher intensity than the rest of the Raman bands in the frequency region. This band is attributed to the C3=C2′ stretching vibration. The corresponding assignment for ICAIO has a very strong Raman band at 1563 cm^{-1} [13]. Due to the absence of the symmetric point of inversion in EBAIO, the corresponding IR band is not expected to be inactive. This can be evidenced from Fig. 1-A, in which the observed IR band at 1572 cm^{-1} contributed by the same vibration mode is rather strong. This observation is similar to that of ICAIO, which has a strong IR band at 1568 cm^{-1} due to the absence of C_i symmetry [13]. The very intense central C=C stretch Raman bands have also been observed and assigned for indigoid dye [16], indigo [17–20], Maya blue [21–24], isoindigo [25], thioindigo and

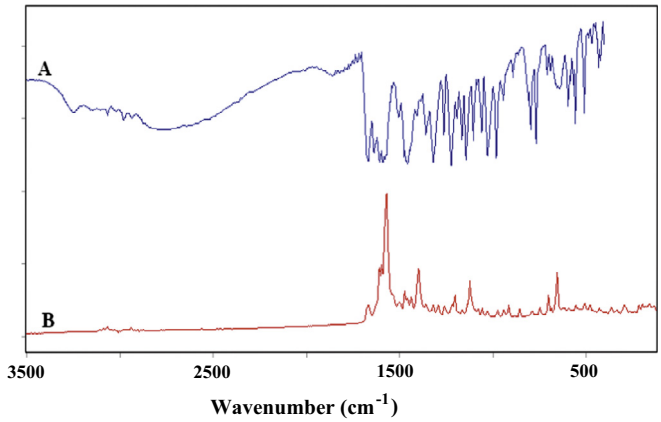

Fig. 1. Vibrational spectra of EBAIO: (A) Infrared; (B) Raman.

indirubin [20] in the frequency region from 1557 to 1594 cm^{-1}. This can be regarded as a characteristic C=C central double bond stretch. The presence of the symmetric point of inversion in indigo and isoindigo makes the absence of the corresponding IR bands due to the activation of exclusion principle. C=O stretch is observed to have a very intense IR band at 1664 cm^{-1} for EBAIO. The corresponding C=O vibration has been assigned to the strong IR bands of ICAIO [13], indigo [17–19,26,27], 4,4,4′,4′-tetramethyl[2,2′-bipyrrolidinylidene]-3,3′-dinone [26] and isoindigo [25] in the frequency range 1630–1730 cm^{-1}. It was pointed out in a FTIR study of 2-pyrrolidinone and oxindole that the lactam carbonyl stretch has lower frequency (1690, 1669 cm^{-1}) in solid than that in vapor phase (1759, 1772 cm^{-1}) and the frequency decreases as the ring size increases [28]. All these should be helpful to confirm our assignment of the carbonyl stretch IR band of EBAIO at 1664 cm^{-1}, which has a corresponding weak Raman band at 1668 cm^{-1}. The relatively low frequency in solid state might be caused by the association with the carbonyl group. The stretches of other double bonds, including the C=C and C=N in the rings and the C=N in the oxime, are expected to have strong or moderate IR intensity. These can be easily identified from the FTIR spectrum in the frequency region between 1572 cm^{-1} (ν(C=C)) and 1664 cm^{-1} (ν(C=O).

The observed FTIR and Raman spectral frequencies are listed in Table 1. The vibrational assignments were suggested based essentially on those of ICAIO [13] except the ethyl group, of which the assignment is referred to group frequency [29,30]. In the FTIR spectrum of EBAIO collected at 24 °C, there was a broad band around 3452 cm^{-1}. This band completely disappeared after baking the sample at 96 °C overnights. This high frequency broad band must therefore be contributed by water presented in the pre-baked sample. Due to the very weak intensity of water Raman band, no water band could be observed in the recorded Raman spectrum. Excluding the water band, the high frequency bands observed in FTIR and Raman spectra are at 3142 and 3148 cm^{-1}, respectively. The spectral frequencies are likely attributed to the N—H stretch in the presence of hydrogen bonding. The fundamental vibrational analysis of pyrrole in the gaseous phase gave the N—H stretch at 3531 cm^{-1} [31,32]. From the experimental condition, it is unlikely that the hydrogen bonding would occur in pyrrole. For pyrroles and indoles, the characteristic frequency of free ν(N—H) is expected to be higher than 3400 cm^{-1}; hydrogen bonding will shift the frequency down to ~3000 cm^{-1} [30]. In the IR spectroscopic study of the association of 2-oxoindolines in solutions, the hydrogen bonded N—H stretch fell in the frequency range 2800–3100 cm^{-1}; the extent of red shift from the free N—H stretch (at 3450 cm^{-1}) depended on the strength of H-bonding and Fermi resonance [33]. For indigo, the intra-hydrogen bonding shifted the observed N—H stretch frequency to 3268 cm^{-1} [17,18]. The observation of ν(N—H) for isoindigo at 3648 cm^{-1} indicated the absence of hydrogen bonding in the molecule [25]. From the molecular structural point of view, the separation between NH hydrogen and carbonyl O could be too far in isoindigo to have any intra-hydrogen bonding. In case of EBAIO, the presence of a moderate IR band at 3142 cm^{-1} and a very weak Raman band at 3148 cm^{-1} is an indication of the occurrence of hydrogen bonding. From the molecular structure of EBAIO, there is a chance of intra hydrogen bonding of N1′H with C2=O. However, the intra-hydrogen bonding is not expected to occur for the oxime hydroxyl group because there is no highly electron negative N or O located in an appropriate nearby location. The free O—H stretch in oxime group is expected to have frequency in the frequency range 3500–3650 cm^{-1} [30]. In the present study, the absence of any IR band in the region and the presence of the red-shift O—H stretch at 3241 cm^{-1} may suggest that the presence of inter-hydrogen bonding in solid EBAIO. Such inter-molecular hydrogen bonding may also occur with the N—H group. Thus, EBAIO molecules associate with each other through hydrogen bonding in solid state. Similar to ICAIO, many observed EBAIO vibrational bands are contributed by mixing different internal vibrations. For simplicity, only the major contributors to the vibrational bands are given in the Table.

In addition to the O—H and N—H stretches, C—H stretch is expected to have vibration in the high frequency region. For both EBAIO and EIM, one my classify C—H into two different types of bonding based on the relative amount of p-orbital in the carbon atom. The first one or type one includes the carbon with ~33% p-orbital in the conjugate ring system; the second one or type two comprises the carbon with ~25% p-orbital in the alkyl chain. Microwave spectroscopic studies have determined the significant difference of bond length between these types of C—H bond. For examples, C—H bonds in pyrrole belong to type one and have bond lengths of 1.076 ± 0.004 Å [34] while C—Hs in propane belong to type two and have bond lengths of 1.096 ± 0.002 Å [35]. From the experimental bond lengths, one may suggest that the C—H bond order of type one is slightly higher than that of type two. This is in agreement with the results of vibrational study, in which of the C—H stretches of pyrrole in the gaseous state fall in the range from 3118 to 3149 cm^{-1} [32] and the corresponding vibrations of propane have frequencies in the range 2882–2977 cm^{-1} [36]. It was also noted that the frequencies of pyrrole in the liquid state are about 15 cm^{-1} lower than those in solid [32]. One may thus expect that the C—H stretch of type one is higher than that of type two. Our observed FTIR bands at 3100, 3062 and 3020 cm^{-1} are assigned to the C—H stretches in the ring. On a similar basis, the

Table 1
Observed vibrational frequencies (cm^{-1}) and suggested assignments of N1-ethyl-5′-bromo-7-azaindirubin-3′-oxime (EBAIO) and N1-ethyl-5′-indirubin-3′-monoxime (EIM).

EBAIO			EIM
FTIR	Raman	Assignments	FTIR
3241 m	3240 vw	ν(OH)H-bonding	3260 w
	3207 vw		
3142 m	3148 vw	ν(NH)H-bonding	3143 m
	3137 vw		3114 m
	3125 vw		
3100 m	3106 vw	ν(C4H)pyr	3100 m
3062 m	3080 w	ν(CH)ring	3058 w
3020 w,b	3062 w	ν(C6′H,C7′H)i	3044 w
	3027 vw		
2975 m	2979 vw	$\nu_a(CH_3)$	2987 m
	2971 vw		
2934 m	2934 w	$\nu_a(CH_2)$	2939 w
	2918 vw		
	2904 vw	$\nu_s(CH_3)$	2894 vw
2870 m,sh		$\nu_s(CH_2)$	2840 m
2778 m,b			
1664 s	1668 w	ν(C=O)	1645 m
1632 m			
1610 m,sh	1608 m	ν(C=C),ν(C=N)ox, or ν(C=N)pyr	1614 s
1602 s	1608 m	ν(C=C)ind	1596 s
1587 s	1597 m	ν(C=C),ν(C=N)ox, or ν(C=N)pyr	1586 s
1572 s	1571 vs	ν(C=C)Z	1564 s
	1550 w	$\delta(CH_3)$ or $\delta(CH_2)$	
1503 w	1500 w	$\delta(CH_3)$	
1472 m	1472 m	$\delta_a(CH_3)$	1480 m
1461 s		β(C7′H,NH)o β(CH,NH)o, ν(CN)ind	1468 s
1456 s		β(CH,NH)o, ν(CN)ind	1453 s
1440 m,sh	1438 m	β(C7′H, NH)o	1435 m
1430w,sh			
1404 w	1400 m	β(CI2H), ν(ring)pyr	1407 w
1380 vw		$\delta_s(CH_3)$	1388 vw
1359 m	1350 vw	β(CI2H),β(C6′H,NH)o, β(OH)	1365 m
1350 m		δ(CH)	
1317 s	1319 w	β(CH,OH)	1334 s
			1301 w
	1293 w	β(C5H,C6H)o, ν(ring)pyr	1288 vw
1261 m	1260 w	β(CI2H), ν(ring)pyr	1280 vw
1221 s	1213 w	β(CH)pyr/ν(ring)ben	1230 s
1190 w	1204 w	ν(ring)ind,β(C4′H,C7′H)o, β(OH)	1192 w
1163 m	1150 w	β(C6′H,C7′H)o, β(NH)	1164 m
			1150 w
1141 s		β(C6′H,C7′H)o, β(NH),	1137 s
1126 vw	1123 m	β(C4H,C5H)o	1120 w
1113 vw		β(C6′H,C7′H), δ(CH)et	
1099 m		β(C6′H,C7′H), δ(CH)et	1092 w
1081 vw	1080 vw	β(C4H, C6H)	1082 vw
1067 w		β(CH)ben	1066 vw
1058 m	1058 vw	β(CH)ben	1030 w
1026 m	1020 vw	β(CH)ind/β(CH)pyr, β(OH)	998 m
982 s	977 w	ν(NO), β(CH)ben	976 w
945 w	940 vw	ν(ring)pyrr, ν(NO)	944 vw
			937 vw
			927 vw
910 w		β(NH), ν(ring)	910 vw
888 w		β(NH), ν(ring)	
859 vw	858 w	δ(CC)et, β(CI2H)	854 vw
807 w		ν(CC)et	
794 m	795 vw	β(C6H,C7H)ind	780 w
780 vw		β(C6H,C7H)ind	757 w
765 m		ϕ(C4H,C5H,C6H)pyr	746 m
755 vw	750 w	φ ring)ben, φ(ring)pyr	
707 vw	706 m	φ (NH), φ(C7H)	730 w
701vw,sh		ν(CBr)	698 vw
688 vw		β(ring)pyr	689 vw
667 w		β(ring)ben, β(ring)pyr	670 vw
655 w	657 m	φ (NH)	
631 w	620 vw	β(NO), β(ring)ind, β(ring)pyr	629 w
598 w	594 vw	β(NH,C7H)out-of-phase	608 w
585 vw		Conformer	588 vw
569 vw	570 vw		574 vw
558 m	555 vw	β(ONC), β(ring)ben	556 w
		β(ring)ben	546 w
510 m	509 w	ϕ(C4′H,C6′H,C7′H), τ(OH)	500 w
480 vw)	480 w	β(ring)pyr/β(ring)ben	
467 vw	466 vvw	ϕ(C4H)	456 vw
433 vw	430 vw	δ(CCN1)	
424 vw		ϕ(C4H)	
418 vw	419 vvw,sh	β(ring)ind, β(CNO)	
404 vw	400 vvw	τ(OH)	
	367 vw		
	339 vvw		
	296 vw		
	210 vw		
	199 vw		
	164 vw		

Abbreviations: s, strong; m, moderate; w, weak; v: very; b, broad; sh, shoulder; ind, indoline; me, methyl; ox, oxime; ben, benzene ring; pyr, pyridine; pyrr, pyrrolidinone; ind, indole; et, ethyl group; Z, central ethylene; ν, stretch; δ, deformation; β, in-plane bend; φ, out-of-plane bend; i, in phase; o, out-of-phase; ω, wag; skel, skeletal;.

observed bands at 2870, 2934 and 2975 cm^{-1} are attributed to the stretches in the ethyl group. The identifications of representation or symmetry agree with those of characteristic group frequencies [29,30].

Displayed in Fig. 2 are the FTIR spectra of EBAIO after the treatments at different temperatures. The upper figure covers the spectra with the frequency range from 2500 to 3500 cm^{--1} and the lower figure from 400 to 2000 cm^{-1}. In both the upper and lower figures, spectra A, B and C were recorded for samples after the treatments at 96, 165 and 225 °C, respectively, for three hours. As there is no spectral variation among these three spectra, the sample of BEAIO is stable up to 225 °C. Spectrum D was collected for the sample after baking at 257 °C. Some variations of spectrum D from spectrum A, B or C in the frequency region from 1550 to 1750 cm^{-1} indicate that the sample begin to have a chemical conversion around 257 °C; but the thermal conversion has not yet completed. Not much change of the spectrum has been observed when the sample was heated up to 274 °C (not shown in the figure). Further heating of the sample up to 300 °C or higher shows a significant change of the spectrum from the one recorded at low temperature. Consequently, there is a possibility of slow kinetics in the thermal conversion. In the high frequency region, three IR bands at 2975, 2934 and 2871 cm^{-1} are clearly observed even after baking the sample at 300 °C. As these three peaks are attributed to the vibrations of C—H stretches in the ethyl group, the decomposed product of EBAIO may still be composed of ethyl group.

To identify the existence of conformer in EBAIO, we have applied a liquid nitrogen cell to record the FTIR spectra at low temperatures. Depicted in Fig. 3 are the FTIR spectra collected at 24, −110 and −196 °C along with the one recorded at room temperature after annealing at 140 °C for three hours (see Spectrum A). Spectrum B was collected with liquid nitrogen cell without annealing the sample at high temperature. It is seen that these two spectra are very similar in both frequency and relative intensity. However, in comparison with those of Spectra C and D collected at −110 and −196 °C, respectively, we have noticed a change of relative intensities for the bands at 598 and 587 cm^{-1}. The relative intensity of the band at 587 cm^{-1} increases with lowering the sample temperature. Consequently, this band is contributed by the low-energy conformer. The spectral quality does not allow us to determine ΔH between the conformers. Similar conformer bands were also identified in the temperature variation study of ICAIO [13]. There are two asymmetric tops in EBAIO. The potential energy

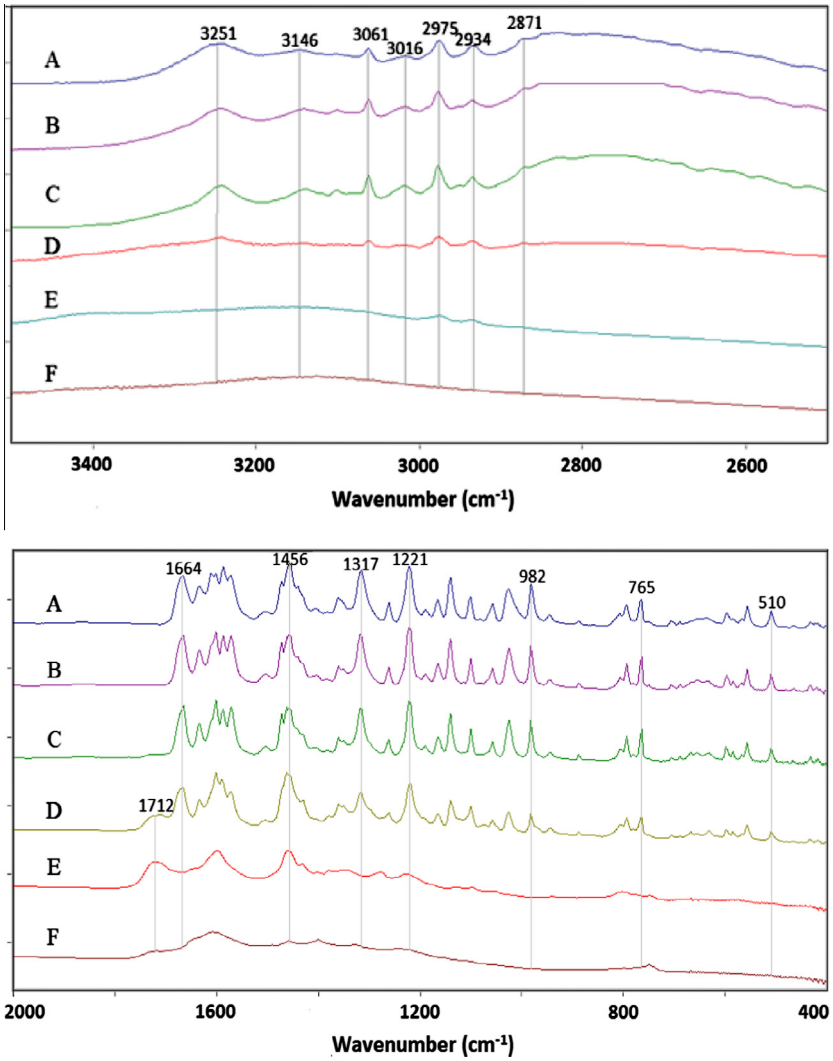

Fig. 2. FTIR spectra of EBAlO after annealing for three hours at different temperatures: (A) 96 °C; (B) 165 °C; (C) 225 °C; (D) 257 °C; (E) 300 °C; (F) 325 °C.

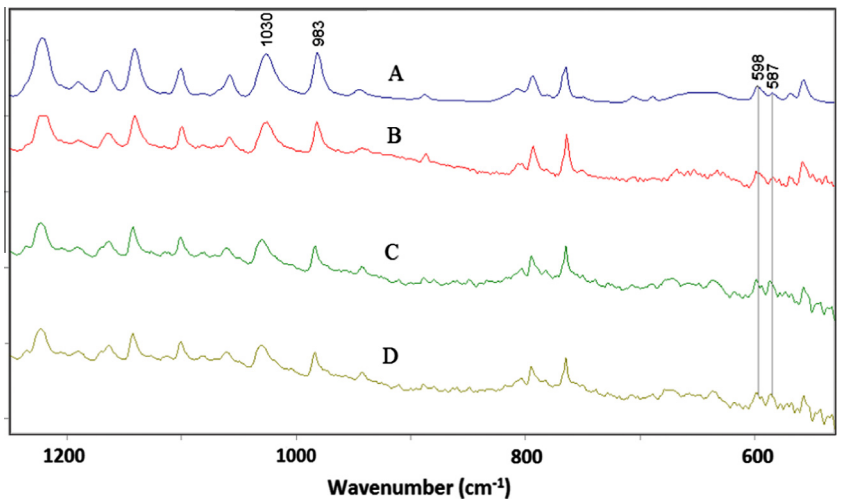

Fig. 3. Variation of EBAlO FTIR spectrum with temperature: (A) 140 °C; (B) 24 °C; (C) −110 °C; (D) −196 °C.

governing the internal rotation of the oxime hydroxyl group is expected to be similar with that of ICAlO. Result from the calculation for ICAlO gave an energy difference of 6.9 kCal/mol between the conformers with the orientations of 0° and 180° for the hydroxyl group. Such a large energy difference gives the population of the high energy conformer to be 0.001% according to Boltzmann

distribution. Thus, it is unlikely that one could identify the conformation due to the internal rotation of hydroxyl group from IR spectroscopy. Consequently, the observation of conformer from the FTIR spectral intensity variation with temperature must arise from the conformer due to the internal rotation of ethyl group.

IR spectra of EIM

EIM has essentially the same ring system as EBAIO except that the N7 in EBAIO is replaced by carbon and the substitution of C5′ bromine in EBAIO by H (see Scheme 1). Thus, the basic ring structure of EIM is similar to that of EBAIO. Depicted in Fig. 4 are FTIR spectra of EIM recorded at room temperature and after the thermal treatments at 96, 170, 257 and 300 °C. As the treatment temperature has increased up to 257 °C, the recorded spectrum D appears to be different from those annealed at lower temperature (see Spectra A, B and C in Fig. 4). Thus one may conclude that EIM has begun to decompose around 257 °C. We have also collected the FTIR spectrum of residue sample obtained after heating up to 400 °C in the DSC experiment. The resulted spectrum is the same as Spectrum E. From the collected IR spectra of samples after the thermal treatment at different temperatures, the decomposition temperature of EIM is roughly the same as that of EBAIO. As the observed IR spectral frequencies of EIM at room temperature are essentially equivalent with those of EBAIO, it is convenient to list the frequencies in Table 1 showing the equivalence of vibration assignments.

In the high frequency region, the highest frequency band at 3465 cm^{-1} appears to be very weak with a broad background. This frequency is relatively low in comparison with both the free N—H stretch around 3648 cm^{-1} [25] and the free O—H stretch of oxime group in the range 3500–3650 cm^{-1} [30]. As the carbonyl stretch overtone has been characterized as a weak IR band in the region 3550–3200 cm^{-1} [30], it is not unreasonable to consider this high frequency weak band as the first overtone of ν(C═O). The appearance of this overtone depends on the anharmonicity of the vibration, and the observed frequency can be different from the twice frequency of the fundamental vibration. However, repeat experiments have shown that the weak band disappeared upon a long time heating of EIM. It is, therefore, suggested that the band is attributable to the water vibration, which is similar to the case, observed in the FTIR spectrum of EBAIO. Other weak or very weak bands observed at 3260, 3114, 3110, 3058, 3044, 2987, 2939, and 2840 cm^{-1} appear to find the corresponding peaks in the FTIR spectrum of EBAIO. Similar assignments are consequently made for the vibrations listed in Table 1. Around the broad band at 3114 cm^{-1}, two partially resolved bands at 3143 and 3100 cm^{-1} could be identified; so is the very weak shoulder (3058 cm^{-1}) located in the high frequency side of the band at 3044 cm^{-1}. The one with relatively higher frequency around 3143 cm^{--1} may arise from the N—H stretch involving with H-bonding; the other bands at 3100, 3058 and 3044 cm^{-1} can be attributed to the C—H stretches of the rings. From Fig. 4, it is noticeable that three bands at 2987, 2939 and 2840 cm^{-1} are forming a pattern similar to that of EBAIO in Fig. 2. Assignments of these three bands may therefore be made to asymmetric CH_3, asymmetric CH_2 and symmetric CH_2 stretches, respectively. These assignments are consistent with the characteristic frequencies expected for the C—H stretches in ethyl group. Furthermore, a very weak shoulder appears on the high frequency side of $\nu_s(CH_2)$. As symmetric CH_3 stretch is generally expected to have a higher frequency than $\nu_s(CH_2)$ [29,30], this weak shoulder band at 2894 cm^{-1} is assigned to $\nu_s(CH_3)$. Although we were unable to observe the corresponding vibration in the IR spectrum of EBAIO, a very weak EBAIO Raman band at 2904 cm^{-1} was observed and assigned to the same vibration. From Fig. 4, it is of interest to note that the C—H stretches of ethyl group present not only in the spectra of samples after the treatments at 24, 96 and 170 °C, but also in the spectrum of thermal conversion product at 257 or 300 °C (see spectra D and E). This result may indicate the existence of ethyl group in the decomposition product of EIM similar to the case of EBAIO.

In the frequency region between 1650 and 1550 cm^{-1}, a moderate band at 1645 cm^{-1} is attributed essentially to the carbonyl stretch. This is equivalent to the assignment of the intense IR band of EBAIO at 1664 cm^{-1}. Other strong bands in this region, including those at 1614, 1596, 1586 and 1564 cm^{-1}, can find the equivalent bands in the FTIR spectrum of EBAIO and are contributed by the C═C and C═N stretches or the combination of these. CH_3 deformation has been characterized to have moderate and strong intensity in the frequency region 1440–1475 cm^{-1} [29]. One may thus assign this moderate band at 1480 cm^{-1} to $\delta(CH_3)$. Many C—H in-plane bending vibrations have been characterized to have frequencies near the range from 976 to 1468 cm^{-1} [29,30]. Consequently, in the FTIR spectrum of EIM, the observed intense or moderate bands at 1334, 1230, 1137 and 998 cm^{-1} are good candidates of these vibrations. The group frequencies of C—H out-of-plane bending vibrations are expected to have frequency in the lower frequency region [30].

Fig. 5 displays the FTIR spectra of (A) ICAIO, (B) EBAIO, (C) EIM and (D) indirubin. The vertical or nearly vertical lines in the figure

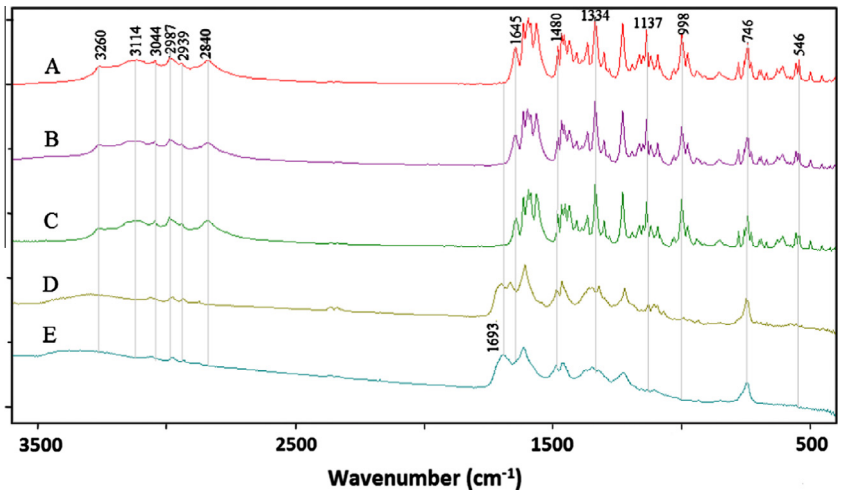

Fig. 4. FTIR spectra of EIM after annealing for three hours at different temperatures: (A) 96 °C; (B) 170 °C; (C) 225 °C; (D) 250 °C; (E) 300 °C.

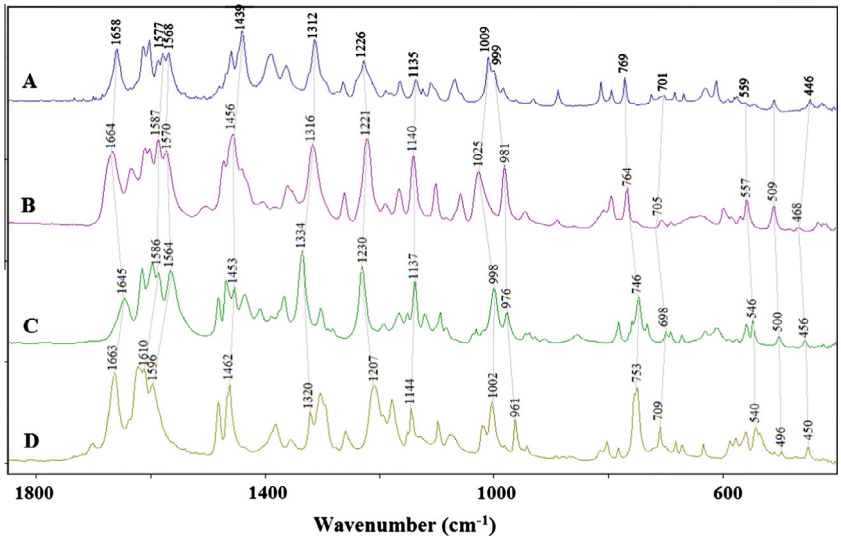

Fig. 5. The correspondence of vibrational modes among the FTIR spectra of (A) ICAIO; (B) EBADO; (C) EIM; (D) indirubin.

are used to show the correlations among the vibrational modes of these molecules. The equivalences of vibrational assignments are reasonable for those bands of different intensities. For each of these four compounds, the C═O stretching band appears to be intense in the frequency range 1645–1664 cm^{-1}. These stretching frequencies are lower than those of aliphatic ketones and five or six-member ring lactone [29,30]. McDermott has carried out the vibrational studies and normal coordinate analyses of γ-butyrolactone, 2-pyrrolidinone and N-methyl-2-pyrrolidinone and assigned the C═O stretches to the strong IR bands at 1770, 1650 and 1670 cm^{-1}, respectively [37]. The relatively high frequency in the lactone compared with those of pyrrolidinones could not be attributed to the intra-hydrogen bonding because the large separation between the amino hydrogen and the O (~2.54 Å) makes it unlikely that this would occur. However, according to the reported potential energy distribution (PED), ν(C═O) is 90.3% for γ-butyrolactone while only 37.3% and 51.4% for 2-pyrrolactone and N-methyl-2-pryyolidinone, respective [37]. PED might therefore be a factor contributing to the difference of C═O stretch frequencies. Additionally, there could be other factors lowering the C═O stretching frequency: One is the hydrogen bonding with N1′—H, which can be evidenced from the red-shift of ν(N1′—H); another is the increasing conjugation with carbonyl group due to the fusion of one conjugation ring or the double bond connection of the pyrrolidinone with another polyaromatic ring.

Thermal measurements

Thermal analyses have been carried out for samples EBAIO and EIM. For comparison, we have also measured the DSC curve for ICAIO. Displayed in Fig. 6 are the DSC curves for these three samples. The chemical conversions for all these samples are observed to be exothermic. Based on the experimental plots, the exothermic conversion temperatures are determined to be 282, 276 and 271 °C, and the enthalpy changes for the chemical conversions are obtained to be −93, −94 and −94 kJ/mole for ICAIO, EBAIO and EIM, respectively. In the thermal measurements, the samples were heat-scanned from 0 to 400 °C after baking out moisture and reaching thermal equilibrium. In separated experiences, the reversed scan from 400 to 0 °C failed to show endothermic conversion; neither exothermic nor endothermic process could be observed in the second upward scan from 0 to 400 °C. All these

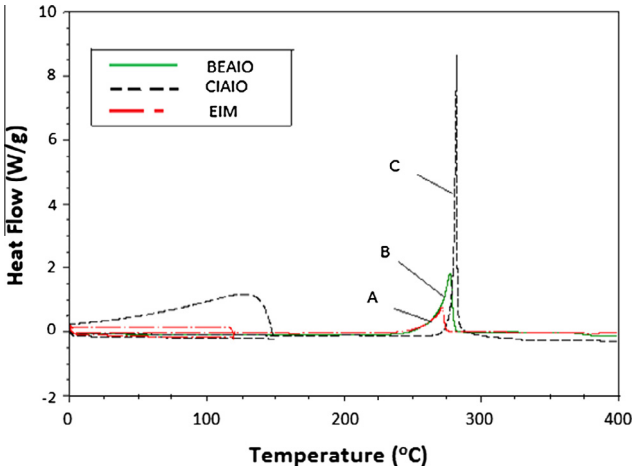

Fig. 6. DSC curves of (A) EIM; (B) EBAIO; (C) ICAIO.

indicate that the exothermic conversions are irreversible processes under our experimental condition. The present DSC experiments have provided more accurate determination for the temperature of chemical conversion. The experimental conversion temperatures determined for all three samples fall in a narrow temperature near 276 ± 6 °C, and the enthalpies of conversion are not significantly different. From the shapes of exotherms, it appears that the kinetic rates of conversion for both EBAIO and EIM are slower than that of ICAIO. The evidence of such slow conversion rate might also be observed from the IR spectra of EBAIO and EIM after the treatments at different temperatures. The chemical conversion temperature of EBAIO has been measured to be 5 °C higher than that of EIM. Such a small difference could not be accurately confirmed from our present IR spectroscopic data.

Summary

In the present study, we have synthesized EBAIO and identified with IR, NMR, MS and elementary analysis. FTIR and Raman spectra of EBAIO and EIM have been recorded and vibrational assignments have been suggested based on the previous work on ICAIO and the group characteristic frequencies. The temperature variation study of IR spectra has identified the presence of two conformers in

EBAIO. A series of FTIR spectra of EBAIO and EIM after baking at different temperatures have been collected. It was found that both EBAIO and EIM begin to decomposed around 257 °C. Thermal analysis has confirmed these results and determined the enthalpies of chemical conversion to be −94 kJ/mol for both EBAIO and EIM.

References

[1] S.P. Williams, P. Shante, M.O. Nowicki, F. Liu, R. Press, J. Godlewski, M. Abdel-Rasoul, B. Kaur, S.A. Fernandez, E.A. Chiocca, S.E. Lawler, Cancer Res. 71 (2011) 5374–5380.
[2] G. Eisenbrand, F. Hippe, S. Jakobs, S. Muehlbeyer, J. Cancer Res. 13 (2004) 627–635.
[3] C. Hoessel, S. Leclerc, J.A. Endicott, M.E. Nobel, A. Lawrie, P. Tunnah, M. Leost, E. Damiens, Nat. Cell Biol. 1 (1999) 60–67.
[4] D. Marko, S. Schatzl, A. Friedel, A. Genzlinger, H. Zankl, J. Cancer Res. Clin. Oncol. 130 (2004) 627–635.
[5] D. Marko, S. Schatzl, A. Friedel, A. Genzlinger, H. Zankl, Br. J. Cancer 84 (2001) 283–289.
[6] F.G.E. Perabo, C. Frossler, G. Landwehrs, D.H. Schmidt, A. Von Rucker, A. Wirger, S.C. Muller, Anticancer Res. 26 (2006) 2129–2135.
[7] K. Ravichandran, A. Pal, R. Ravichandran, Microsc. Res. Tech. 73 (2010) 1053–1058.
[8] E.A. Perpete, J. Preat, J.-M. Andre, D. Jacquemin, J. Phys. Chem. A 110 (2006) 5629–5635.
[9] B.-X. Ye, L.-J. Yuan, C. Chen, J.-C. Tao, Electroanalysis 17 (2005) 1523–1528.
[10] T. Karapanayoitis, S.E. Jorge, Analyst 129 (2004) 613–618.
[11] Y.-S. Li, J. Church, J. Food Drug Anal. 22 (2014) 29–48.
[12] Y.-S. Li, J. Cheng, K.T. Chung, Spectrochim. Acta Part A 69 (2008) 524–527.
[13] T. Robbins, Y. Wang, Q.-Z. Yao, Z.-H. Wang, J. Mol. Struct. 1048 (2013) 51–58.
[14] J. Tatsugi, T. Zhiwei, Y. Izawa, Arkivoc 1 (2001) 63–73.
[15] D. Raileanu, O. Constantinescu-Simon, E. Mosanu, C.D. Nenitzescu, Rev. Roum. Chim. 12 (1967) 105–108.
[16] A.V. Barnov, Y.S. Bobovich, V.I. Petrov, Opt. Spectrosc. 61 (1986) 315–319.
[17] E. Tatsch, B. Schrader, J. Raman Spectroc. 26 (1995) 467–473.
[18] A. Amat, F. Rosi, C. Miliani, A. Sgamellotti, S. Fantacci, J. Mol. Struct. 993 (2011) 43–51.
[19] E.-S. Min, S.I. Nam, M.S. Lee, Bull. Chem. Soc. Jpn. 75 (2002) 677–680.
[20] I.V. Aleksandrov, Spectroscopy 45 (1978) 341–342.
[21] M.S. del Rio, M. Picquar, E. Haro-Poniatowski, E. van Elslande, V.H. Uc, J. Raman Spectrosc. 37 (2006) 1046–1053.
[22] P. Vandenabeele, S. Bode, A. Alonso, L. Moens, Spectrochim. Acta, Part A 61 (2005) 2349–2356.
[23] H.G. Wiedemann, K.-W. Brzezinka, K. Witke, I. Lamprecht, Thermochim. Acta 456 (2007) 56–63.
[24] A. Domenech, J. Raman Spectrosc. 42 (2011) 86–96.
[25] S. Lunak, Chem. Phys. Lett. 477 (2009) 116–121.
[26] E. Wille, W. Luttke, Liebigs Ann. Chem. 12 (1980) 2039–2054.
[27] D.N. Shigorin, N.S. Dokunikhin, E.A. Gribova, Z. Fiz, Z. Fiz. Khim. 29 (1955) 867–876.
[28] W.M. Coleman III, B.M. Gordon, Appl. Spectrosc. 42 (1988) 108–113.
[29] D. Lin-Vien, N.B. Colthup, W.G. Fateley, J.G. Grasselli, The Hand Book of Infrared and Raman Characteristic Frequencies of Organic Molecules, AP, Boston, 1991.
[30] G. Socrates, Infrared and Raman Characteristic Group Frequencies, third ed., John Wiley and Sons, Chichester, 2001.
[31] D.W. Scott, J. Mol. Spectrosc. 37 (1971) 77–91.
[32] T.D. Klots, R.D. Chirico, W.V. Steele, Spectrochim. Acta, Part A: Mol. Biomol. Spectrosc. 50A (1994) 765–795.
[33] A. Koll, M. Rospenk, L. Stefaniak, J. Wojcik, J. Phys. Org. Chem. 7 (1994) 174–177.
[34] L. Nygaard, J.T. Nielsen, J. Kirchheiner, G. Maltesen, J. Rastrup-Andersen, G.O. Sorensen, J. Mol. Struct. 3 (1969) 491–506.
[35] D.J. Lide, J. Chem. Phys. 33 (1960) 1514.
[36] T. Ogawa, J. Hara, K. Hirota, Nippon Kaga. Z. 89 (1968) 19–22.
[37] D.P. McDermott, J. Phys. Chem. 90 (1986) 2569–2574.